THE DEVELOPMENT OF TWO MULTIAXIAL DUCTILITY FACTOR PREDICTING MODELS BASED ON CREEP CAVITY GROWTH THEORY

Dongquan Wu, Yupeng Li, Zixiang Liu, Dinghe Li

Sino-European Institute of Aviation Engineering, Civil Aviation University of China, Tianjin, China

corresponding author Dongquan Wu, e-mail: dqwu@cauc.edu.cn

In this study, the multiaxial ductility factor was analyzed based on the power-law creep grain-boundary cavities growth theory under multiaxial stress states. Based on this theory, the theoretical cavities growth rates under a multiaxial stress state were discussed and the predicting model of a stress-state parameter α was revised by using an empirical fitting expression denoted as α_{Wu}, which exhibited a good agreement to analytical results of the stress-state parameter α and multiaxial cavities growth rates. Then, according to the relationship between uniaxial and multiaxial creep failure strain, a new empirical predicting model of multiaxial ductility factor MDF_{Wu} was established which involved the multiaxial parameter α_{Wu} and uniaxial parameter α_0. Besides, the theoretical model of multiaxial ductility factor MDF could also be established. By fitting the theoretical values of MDF, another predicting model MDF_{WM} was proposed. The development of two multiaxial ductility factor predicting models could be achieved. Finally, predictions of these two novel multiaxial ductility factor models and the Cocks-Ashby as well as Wen-Tu model were compared with experimental data, and the prediction accuracy of MDF_{Wu} and MDF_{WM} models was significantly improved, especially for the latter one.

Keywords: multiaxial ductility factor, cavities growth theory, power-law creep, multiaxial stress state

1. Introduction

Metallic components in modern industrial core equipment (such as aero engines, ultra supercritical generator sets, nuclear motor sets, etc.) are subjected to higher temperature in order to realize the continuous improvement of energy conversion efficiency. Thus, creep cracking is one of the most important failure mechanisms of these components, especially when containing precracks, which will cause failures before their design life (Yatomi *et al.*, 2004). A large number of theories and experiments have proved that creep crack initiation and propagation are the main causes of structural failure in service (Holdsworth, 1992).

For safety reasons, the structural integrity assessment of components operating in the creep regime is imperative (Wen and Tu, 2014). The analysis of creep cracking and failure based upon continuum damage mechanics has made a remarkable development in recent years, which makes up for deficiency of fracture mechanics (Wen and Tu, 2014). Within this approach, the creep cracking process will be directly correlated to the creep damage described by a damage variable around the crack tip. Once the damage variable of one material point reaches the critical value, it is thought to be failed, and the crack growth length can be measured by the whole damaged area. To effectively describe the complex stress state around the crack tip, for example, the stress state around the crack tip of a compact tension specimen should be a multiaxial distribution. A multiaxial ductility factor (MDF) is usually used to build the relationship between the multiaxial ductility ε_f^* and uniaxial ductility ε_f

$$\varepsilon_f^* = MDF \varepsilon_f \tag{1.1}$$

To effectively characterize the relationship between them, various multiaxial ductility factor (*MDF*) models were proposed, which can be roughly divided into the following bases: empirical formula; semi-empirical formula; physical mechanisms.

For empirical formula, Manjoine (1975) proposed an *MDF* model which was inversely proportional to triaxiality according to mechanical performance of annealed 304 stainless steel

$$MDF = \frac{\varepsilon_f^*}{\varepsilon_f} = \frac{\sigma_{eq}}{3\sigma_m} \tag{1.2}$$

where σ_m and σ_{eq} are the hydrostatic stress and von Mises equivalent stress, respectively.

For a semi-empirical formula, Spindler (2004) modified the Rice-Tracey *MDF* model (Rice and Tracey, 1969) and developed a semi-empirical *MDF* model considering the nucleation and growth of creep voids

$$MDF = \frac{\varepsilon_f^*}{\varepsilon_f} = \exp\Big[p\Big(1 - \frac{\sigma_1}{\sigma_e}\Big) + q\Big(0.5 - 1.5\frac{\sigma_m}{\sigma_{eq}}\Big)\Big] \tag{1.3}$$

where σ_1 is the principal stress, and p and q are material coefficients.

For the *MDF* model based on physical mechanisms, different mechanisms such as cavity growth (Rice and Tracey, 1969; McClintock, 1968; Cocks and Ashby, 1980) and cavity nucleation (Spindler, 2004a,b) have been discussed. Typically, Cocks and Ashby (1980) proposed a creep model based on micromechanical consideration of the void growth and coalescence and extended it to multiaxial stress states as well as the most notable Cocks-Ashby *MDF* models

$$MDF = \frac{\varepsilon_f^*}{\varepsilon_f} = \sinh\Big(\frac{2}{3}\frac{n - 0.5}{n + 0.5)}\Big)\Big/ \sinh\Big(2\frac{n - 0.5}{n + 0.5}\frac{\sigma_m}{\sigma_{eq}}\Big) \tag{1.4}$$

where n is the steady-state creep exponent. Alang and Nikbin (2018) and Spindler *et al.* (2001) also proposed other (semi) empirical models, which may be also suitable for different conditions. Due to perfect establishment and application at the grain size level, the Cocks-Ashby *MDF* has been widely used to estimate the multiaxial creep ductility during simulation or estimation of creep damage (Wen and Tu, 2014; Yatomi and Tabuchi, 2010; Wu *et al.*, 2018b,c,d) and creep cracking life (Davies, 2006; Wu *et al.*, 2018a,e, 2019, 2020). Nevertheless, the Cocks-Ashby *MDF* may conservatively predict multiaxial creep ductility under some conditions. Thus, Wen *et al.* (2014) developed another purely empirical Wen-Tu *MDF* based on the Cocks-Ashby *MDF*, which could more effectively estimate the experimental results

$$MDF = \frac{\varepsilon_f^*}{\varepsilon_f} = \exp\Big(\frac{2}{3}\frac{n - 0.5}{n + 0.5)}\Big)\Big/ \exp\Big(2\frac{n - 0.5}{n + 0.5}\frac{\sigma_m}{\sigma_{eq}}\Big) \tag{1.5}$$

However, the above models are approximate solutions of the theoretical model based on the power-law creep growth of grain-boundary cavities theory, which will be explained in detail in Section 2, and there is a large conservation under some conditions, so it is necessary to establish a more accurate multiaxial ductility factor based on the creep cavity growth model. Therefore, the critical task of the present study is to develop a more accurate *MDF* based on the grain boundary void growth model.

2. Power-law creep regime based on growth of grain-boundary cavities

Experimental morphology from different steels of creep crack growth has indicated that creep voids or cavities mainly nucleate and grow on grain boundary facets (especially when a tensile stress is perpendicular to the facets), then the cavities may be coalescing to form a grain-size

microcrack, and finally the coalescence of microcracks leads to creep crack propagation (Tan *et al.*, 2013; Wen and Tu, 2014; Wen *et al.*, 2016; You and Lee, 1996; Al-Rifaie and Sumelka, 2019; Al-Rifaie *et al.*, 2021).

Cocks and Ashby (1980) proposed an approximate method to calculate the growth of grain-boundary cavities by a power-law creep under multiaxial stress states. In this theory, the cavity growth was estimated by a volume change of the cylinder containing a void, and some strict assumptions should be met, such as grain-boundary cavities grow by a power-law creep. The creep rate is independent of hydrostatic pressure, the grain boundaries and take a relative rigid-body displacement, width of the cylinder is larger than its thickness, and it is constrained by the surrounding material to contract laterally, the voids stay spherical during the creep process, the material is incompressible and its total volume does not change.

The problem then arises with calculation of the volume change in the cylinder containing voids, since they cause the cavities to grow.

A detailed view of a cylinder containing a void is shown in Fig. 1, in which d is the grain size, r_h is the void radius, $2l$ is the voids distance, $2w$ is a calculation bound, σ_a is the axial stress in the cylinder and T is the superimposed triaxial stress.
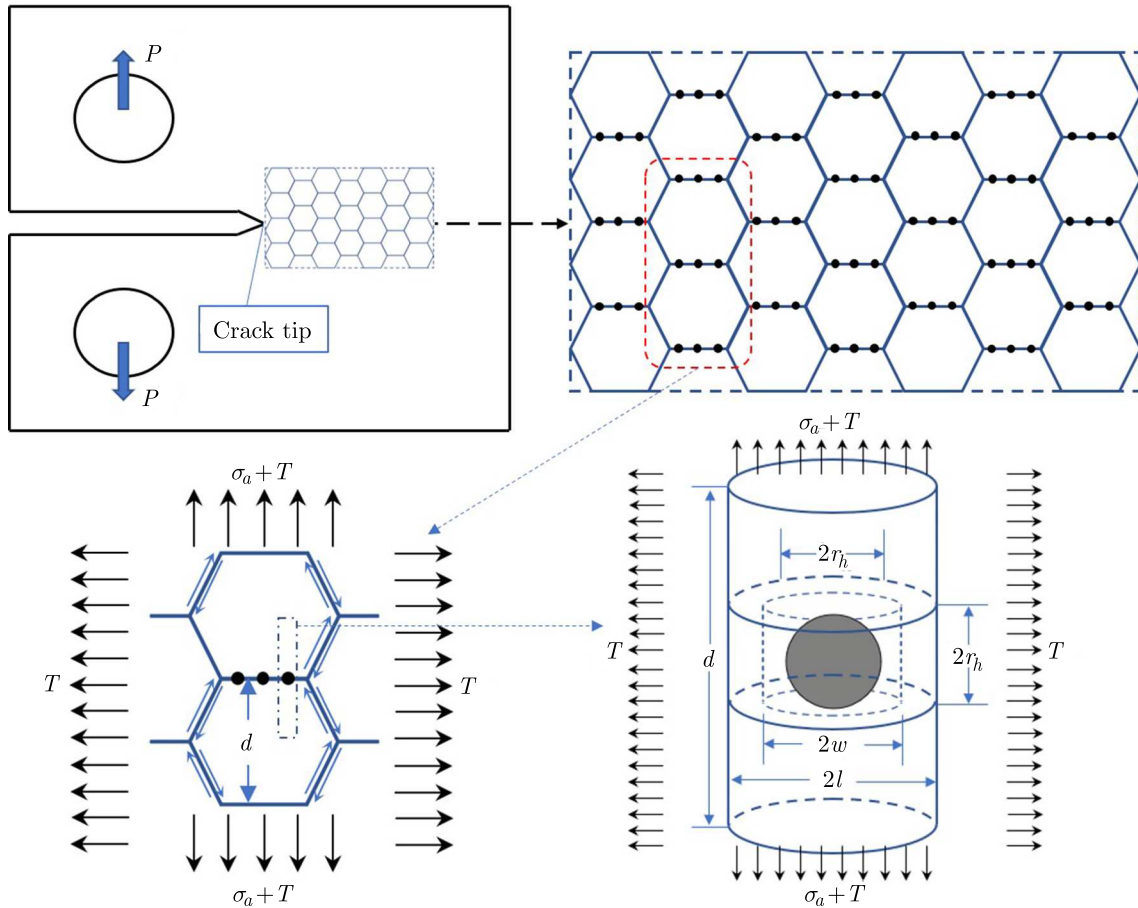
Fig. 1. Grain-boundary cavities growth by a power-law creep under multiaxial stress states

Cocks and Ashby (1980) established the upper bound for the axial strain rate $\dot{\varepsilon}_{ss}$ for uniaxial stress by using the energy principles

$$\frac{1}{1-f_n}\frac{df_h}{dt} = \dot{\varepsilon}_{ss}\Big[\frac{1}{(1-f_h)^{n+1}} - 1\Big] \tag{2.1}$$

where f_h is the area fraction of holes on the grain boundary, $f_w = r_h^2/l^2$, $\dot{\varepsilon}_{ss}$ is the steady creep rate in the absence of voids. And for a multiaxial stress condition, the axial strain rate is described as

$$\frac{df_h}{dt} = \dot{\varepsilon}_{ss}\frac{f_h}{f_w}\left[\frac{\sqrt{(1+G)^{n+1}}}{(1-f_w)^n} - (1-f_w)\right] \tag{2.2}$$

where f_w is an area fraction entering the bound calculation, $f_w = r_h^2/w^2$, and G is a stress-state parameter defined by

$$G = 3\left(\frac{n}{n+1}\frac{1-f_w}{\ln f_w}\frac{T}{\sigma_a}\right)^2 \tag{2.3}$$

The optimum value of f_w was found by minimizing df_h/dt with respect to f_w, with the constraint that f_w cannot be less than f_h. The unconstrained optimum value was found using the Newton-Raphson method.

Be aware of that it is difficult to directly obtain the relationship between the void growth rate and stress triaxiality, and to make the predicting results more practical. Cocks and Ashby (1980) fitted a semi-empirical equation to the curves of Fig. 2. It was fitted by a result which closely resembled that for a imple uniaxial tension condition, Eq. (2.1), namely

$$\frac{df_h}{dt} = \frac{\dot{\varepsilon}_{ss}}{\alpha}\left[\frac{1}{(1-f_h)^n} - (1-f_h)\right] \tag{2.4}$$

where α is a stress-state parameter defined by

$$\alpha = \sinh^{-1}\left[\frac{2(n-0.5)}{n+0.5}\frac{\sigma_m}{\sigma_{eq}}\right] \tag{2.5}$$

As expected, cavity growth rates are increasing with the increasing stress triaxiality. It is also observed from Fig. 5 that the results are not well fitted when the triaxiality $\sigma_m/\sigma_{eq} < 0.8$ or creep exponent $n < 3$. This is mainly because the most weight is artificially given to the predicting results at high stress triaxiality in the Cocks and Ashby fitting process. To resolve this conflict, Wen and Tu (2014) proposed another approximate model formulated as

$$\alpha = \left[2 - 0.5\left(\frac{1}{5n}\right)^{n-1}\right]\Big/\left[\frac{2(n-0.5)}{n+0.5}\frac{\sigma_m}{\sigma_{eq}}\right] \tag{2.6}$$

In the case of simple tension, substituting $\sigma_m/\sigma_{eq} = 1/3$ into Eq. (2.5) or Eq. (2.6) yields the void growth rate under the uniaxial condition with α_0.

Here, we try to propose a new formula for describing the relationship between the parameter α and triaxiality σ_m/σ_{eq}, which is built by fitting the theoretical results.

First, the variations of α_{true} against triaxiality σ_m/σ_{eq} for different n values are obtained from Eq. (2.4) and Eq. (2.2)

$$\alpha_{true} = \left[\frac{1}{(1-f_h)^2} - (1-f_h)\right]\Big/\left\{\frac{f_h}{f_w}\left[\frac{\sqrt{(1+G)^{n+1}}}{(1-f_w)^n} - (1-f_w)\right]\right\} \tag{2.7}$$

Moreover, the theoretical data of α_{true} could be obtained by re-arranging the results from Fig. 3, then the curves of $\ln\alpha_{true}$ against σ_m/σ_{eq} with different n can be described in Fig. 2.

It can be found that α_{true} decreases as n is increasing, and the difference between the curves is unobvious when n is larger than 6. Besides, it is concluded that with the increasing stress triaxiality σ_m/σ_{eq}, the curves of $\ln\alpha_{true}$ against σ_m/σ_{eq} are rapidly decreasing when σ_m/σ_{eq} is smaller than 1.5, while it becomes smooth when σ_m/σ_{eq} is larger than 1.5. By fitting
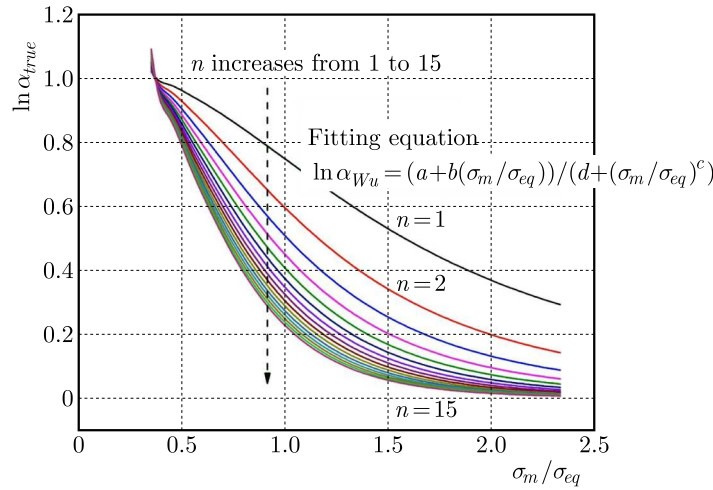
Fig. 2. Variation of the stress-state parameter α_{true} against σ_m/σ_{eq} under different n values

the relationship between the parameter α_{true} and stress triaxiality for different n values, it is indicated that all of the curves could be expressed by a similar type of mathematical expression, and the fitting equation is expressed as follows using the parameter α_{Wu}

$$\ln \alpha_{Wu} = \left[a + b\left(\frac{\sigma_m}{\sigma_{eq}}\right)^c \right] \bigg/ \left[d + \left(\frac{\sigma_m}{\sigma_{eq}}\right)^c \right] \tag{2.8}$$

or expressed by

$$\alpha_{Wu} = \exp \left\{ \left[a + b\left(\frac{\sigma_m}{\sigma_{eq}}\right)^c \right] \bigg/ \left[d + \left(\frac{\sigma_m}{\sigma_{eq}}\right)^c \right] \right\} \tag{2.9}$$

where a, b, c, d are all parameters related to n, which can be also correlated by the following formula by using coefficients a_i, b_i, c_i, d_i. Perfect fitting performance is also found here, and the coefficient of determination R-square is larger than 0.999. These parameters could be obtained directly from Table 1

$$a, c = \frac{a_i + b_i n}{1 + c_i n + d_i n^2} \qquad i \text{ is represented by } a \text{ or } c$$

$$b, d = a_i b_i^{\frac{1}{n}} n^{c_i} \qquad i \text{ is represented by } b \text{ or } d \tag{2.10}$$

Table 1. The details of fitting coefficients (a, b, c, d) between above coefficients against n values

Coef. 1	Coefficient 2			
	a_i	b_i	c_i	d_i
a	0.020863	−0.51239	0.215807	−0.00294
b	0.090558	0.557567	0.57484	–
c	−2.15624	−0.36378	0.227893	0.000304
d	0.30566	0.382147	−0.19855	–

Then the parameter α_{Wu} can be characterized by combining Eqs. (2.9) and (2.10), which is related to the stress triaxiality σ_m/σ_{eq} and n values

$$\alpha_{Wu} = \exp\left\{\left[\frac{a_a + b_a n}{1 + c_a n + d_a n^2} + a_b b_b^{\frac{1}{n}} n^{c_b}\left(\frac{\sigma_m}{\sigma_{eq}}\right)^{\frac{a_c + b_c n}{1 + c_c n + d_c n^2}}\right]\Big/\left[a_d b_d^{\frac{1}{n}} n^{c_d} + \left(\frac{\sigma_m}{\sigma_{eq}}\right)^{\frac{a_c + b_c n}{1 + c_c n + d_c n^2}}\right]\right\}$$

(2.11)

Figure 3 compares the predictions and true values of α for $n = 18$ and $n = 20$, where these two conditions are not considered in the above fitting process, so the comparison between these two conditions and predictions can effectively verify the accuracy of α_{Wu} model in predicting the parameter α.
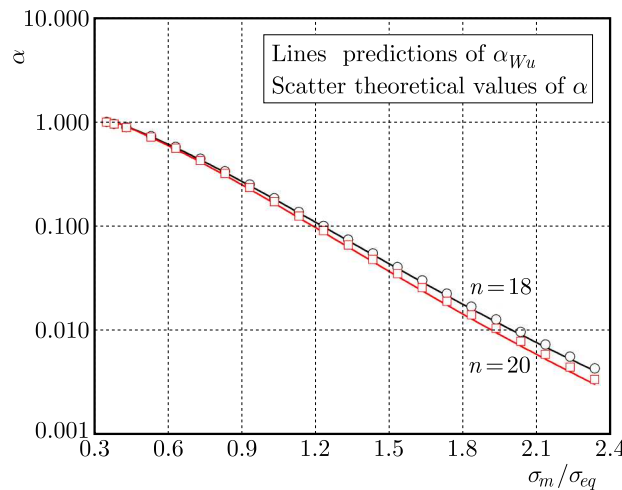
Fig. 3. Comparison between predictions of α_{Wu} and true values of α with $n = 18$ and $n = 20$

Finally, the normalized hole growth rate, $\ln[(df_h/dt)/(1/\dot{\varepsilon}_{ss}f_h)]$ for different n is compared by using different α models (i.e. Cocks-Ashby model in Eq. (2.5), Wen-Tu model in Eq. (2.6) and Wu model in Eq. (2.11)), as shown in Fig. 4. The Cocks-Ashby approximate model shows large conservativeness when $n = 1$, σ_m/σ_{eq} is smaller than 0.5 and n is larger than 5. The Wen-Tu model is relatively more accurate than the Cocks-Ashby approximate model at $n = 1$ and small values of σ_m/σ_{eq}, but its prediction is still much too conservative when n is larger than 5. Apparently, compared with the Cocks-Ashby approximate model and Wen-Tu model, the proposed model (Wu model) is perfectly suitable to predict theoretical data of the hole growth rate no matter how the stress triaxiality σ_m/σ_{eq} or creep exponent n varies. The predictions of Wu model (solid line) nearly coincide with the theoretical data (dash line). Especially, there is a significant improvement for the predicting accuracy when $\sigma_m/\sigma_{eq} < 0.5$ and creep exponent $n > 5$ compared with other models.

The time to fracture at a constant stress is generally obtained by integrating the creep voids growth rate between the limits, and the creep failure strain could be simply assumed by the ratio of the time to fracture and the steady creep rate in absence of voids. And then there are two conditions for assuming the time to failure: one is using theoretical differential equations, the other is using approximate or fitting equations.

The first is using the theoretical differential equations.

To get the creep failure strain under the uniaxial loading condition, differential Eq. (2.1) can be integrated between the limits

$$\begin{aligned} f_h &= f_i & \text{at} & \quad t = 0 \\ f_h &= f_{c0} & \text{at} & \quad t = t_{c0} \end{aligned}$$

(2.12)

where f_i is the initial area fraction of the cavities, which is thought to be $f_i \ll 1$, f_{c0} is the area fraction of the cavities at which the linkage occurs, which is taken to be $f_{c0} = 0.25$ (Wen and
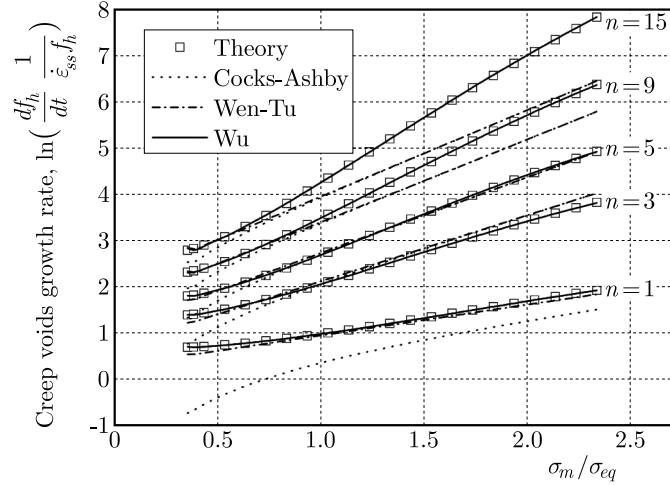
Fig. 4. Comparison of predictions and theoretical results of the creep voids growth rate

Tu, 2014). And t_{c0} is the time to coalescence. The result for a constant stress is an equation for the failure time

$$t_{c0} = \frac{1}{\dot{\varepsilon}_{ss}(n+1)} \ln \frac{1-(1-f_c)^{n+1}}{1-(1-f_i)^{n+1}} \tag{2.13}$$

Then the creep failure strain under a uniaxial loading condition is

$$\varepsilon_f = \dot{\varepsilon}_{ss} t_{c0} = \frac{1}{n+1} \ln \frac{1-(1-f_c)^{n+1}}{1-(1-f_i)^{n+1}} \tag{2.14}$$

To get the creep failure strain under multiaxial loading conditions, differential Eq. (2.2) can be integrated between the limits

$$\begin{aligned} f_h &= f_i & \text{at} & & t = 0 \\ f_h &= f_c & \text{at} & & t = t_c \end{aligned} \tag{2.15}$$

where t_c is the time to coalescence.

For theoretical differential Eq. (2.2) integrated between the above limits, the time to failure could be expressed by

$$t_c = \frac{f_w}{\dot{\varepsilon}_{ss}} \ln \frac{f_c}{f_i} \bigg/ \left[\frac{\sqrt{(1+G)^{n+1}}}{(1-f_w)^n} - (1-f_w) \right] \tag{2.16}$$

Then, the creep failure strain under multiaxial loading conditions is calculated as

$$\varepsilon_f^* = \dot{\varepsilon}_{ss} t_c = f_w \ln \frac{f_c}{f_i} \bigg/ \left[\frac{\sqrt{(1+G)^{n+1}}}{(1-f_w)^n} - (1-f_w) \right] \tag{2.17}$$

Finally, the multiaxial ductility factor (MDF) can be defined as

$$MDF = \frac{\varepsilon_f^*}{\varepsilon_f} = \frac{f_w \ln \frac{f_c}{f_i}}{\ln \frac{1-(1-f_c)^{n+1}}{1-(1-f_i)^{n+1}}} \bigg/ \left[\frac{\sqrt{(1+G)^{n+1}}}{(1-f_w)^n} - (1-f_w) \right] \tag{2.18}$$

In this formula, it is found that except for stress triaxiality σ_m/σ_{eq}, the initial area fraction of the cavities f_i also affects MDF, which will be studied in the following Section.

The other condition for assuming the time to failure is using simplified differential equations. For the multiaxial loading condition, differential Eq. (2.5) can be integrated between the limits, the time to failure could be expressed by

$$t_c = \frac{\alpha}{\dot{\varepsilon}_{ss}(n+1)} \ln \frac{1-(1-f_c)^{n+1}}{1-(1-f_i)^{n+1}} \tag{2.19}$$

The creep failure strain under multiaxial loading conditions is described as

$$\varepsilon_f^* = \dot{\varepsilon}_{ss} t_c = \frac{\alpha}{n+1} \ln \frac{1-(1-f_c)^{n+1}}{1-(1-f_i)^{n+1}} \tag{2.20}$$

For the uniaxial condition, the void growth rate is described as α_0 by substituting $\sigma_m/\sigma_{eq} = 1/3$ into Eq. (2.6). Hence, similarly, the time to failure under this condition is characterized by

$$t_{c0} = \frac{\alpha}{\dot{\varepsilon}_{ss}(n+1)} \ln \frac{1-(1-f_c)^{n+1}}{1-(1-f_i)^{n+1}} \tag{2.21}$$

The creep failure strain under uniaxial loading conditions is calculated by

$$\varepsilon_f = \dot{\varepsilon}_{ss} t_{c0} = \frac{\alpha}{n+1} \ln \frac{1-(1-f_c)^{n+1}}{1-(1-f_i)^{n+1}} \tag{2.22}$$

Finally, the *MDF* can be re-defined as

$$MDF = \frac{\varepsilon_f^*}{\varepsilon_f} = \frac{\alpha}{\alpha_0} \tag{2.23}$$

In our study, according to the new α_{Wu} proposed in Eq. (2.12), the modified *MDF* is described as

$$MDF_{Wu} = \frac{\varepsilon_f^*}{\varepsilon_f} = \frac{\alpha_{Wu}}{\alpha_{Wu0}} = \frac{\exp\left\{\left[a+b\left(\frac{\sigma_m}{\sigma_{eq}}\right)^c\right]\Big/\left[d+\left(\frac{\sigma_m}{\sigma_{eq}}\right)^c\right]\right\}}{\exp\left\{\left[a+b\left(\frac{1}{3}\right)^c\right]\Big/\left[d+\left(\frac{1}{3}\right)^c\right]\right\}} \tag{2.24}$$

where a, b, c, d are all parameters related to n, which are described above.

Figure 5 compares *MDF* results for different predicting models and theoretical data with varied values of f_i. With an increase of f_i, the curves of *MDF* are descended, and these curves are almost coincident when $f_i < 10^{-4}$. The Wu model shows a perfect coincidence with the theoretical results when n is small, while both the Cocks-Ashby and Wen-Tu models are conservative. As the creep power law exponent n increases, the difference between Wu model and theoretical results becomes obvious, especially when the stress triaxiality is smaller than 1. This is mainly caused by simplification using the creep void growth rate with α_0 under the uniaxial tension condition. Compared to the theoretical uniaxial creep void growth rate in Eq. (2.3), α_0 is not equal to 1 in the simplified creep void growth rate Eq. (2.7), and this difference will be enlarged at high n values. Besides, for large n, the difference between Wu and Wen-Tu models is decreased, and the predictions of Wen-Tu model at large n may be overestimated when $\sigma_m/\sigma_{eq} > 1$. Due to relatively poor predictions of these models at large n, a new model for predicting *MDF* should be proposed.

Therefore, a fitting formula for *MDF* is obtained by fitting the theoretical results of *MDF* with $f_i = 10^{-4}$, because the curves of *MDF* are almost coincident when $f_i < 10^{-4}$.

The theoretical results of $\ln MDF$ against σ_m/σ_{eq} with $f_i = 10^{-4}$ for different n are compared. All of the curves could be well fitted by the following equation (WM means modified Wu model)

$$\ln MDF_{WM} = \frac{a+b\left(\frac{\sigma_m}{\sigma_{eq}}\right)^c}{d+\left(\frac{\sigma_m}{\sigma_{eq}}\right)^c} \qquad MDF_{WM} = \exp\left[\frac{a+b\left(\frac{\sigma_m}{\sigma_{eq}}\right)^c}{d+\left(\frac{\sigma_m}{\sigma_{eq}}\right)^c}\right] \tag{2.25}$$
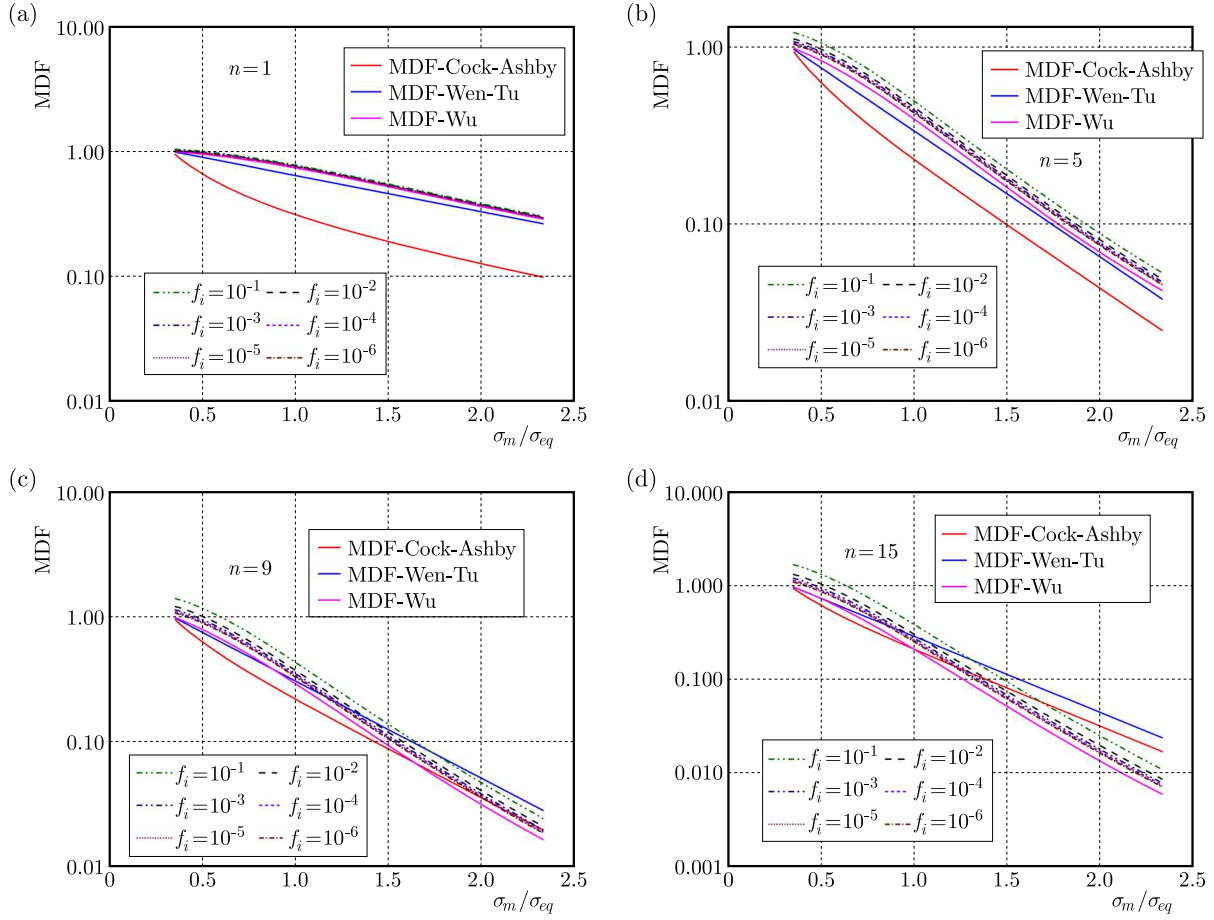
Fig. 5. Comparison of predictions and theoretical results of *MDF*

where a, b, c, d are parameters related to the creep power exponent n, and the following expression could be established

$$a, b, c = \frac{a_i + b_i n}{1 + c_i n + d_i n^2} \qquad i \text{ is represented by } a,\ b,\ c$$

$$d = a_i + b_i + c_i^n + d_i n \qquad i \text{ is represented by } d$$

(2.26)

The related parameters are summarized in Table 2.

Table 2. Fitting parameters of above parameters against n values

Coef. 1	Coefficient 2			
	a_i	b_i	c_i	d_i
a	0.037707	−0.51284	0.228236	−0.00278
b	−0.00624	0.071408	0.085232	−8.17E-04
c	−2.25401	−0.49529	0.29565	−3.88E-04
d	0.194207	−0.17086	0.375464	−0.00112

To further validate the suitability of the modified Wu (WM) model, the *MDF* for $n = 8$, $n = 15$, $n = 18$ and 20 are also compared between different models in Fig. 6. The predictions from the WM model (black solid line) are quite accurate compared to the theoretical data (scatters data), while the other predictions are far below the theoretical data when $\sigma_m/\sigma_{eq} < 0.5$. Note

that $n = 18$ and 20 conditions are not considered in the above fitting process, so the comparison could effectively support the conclusion that the WM model could be the most competitive theory in assessing the *MDF*.
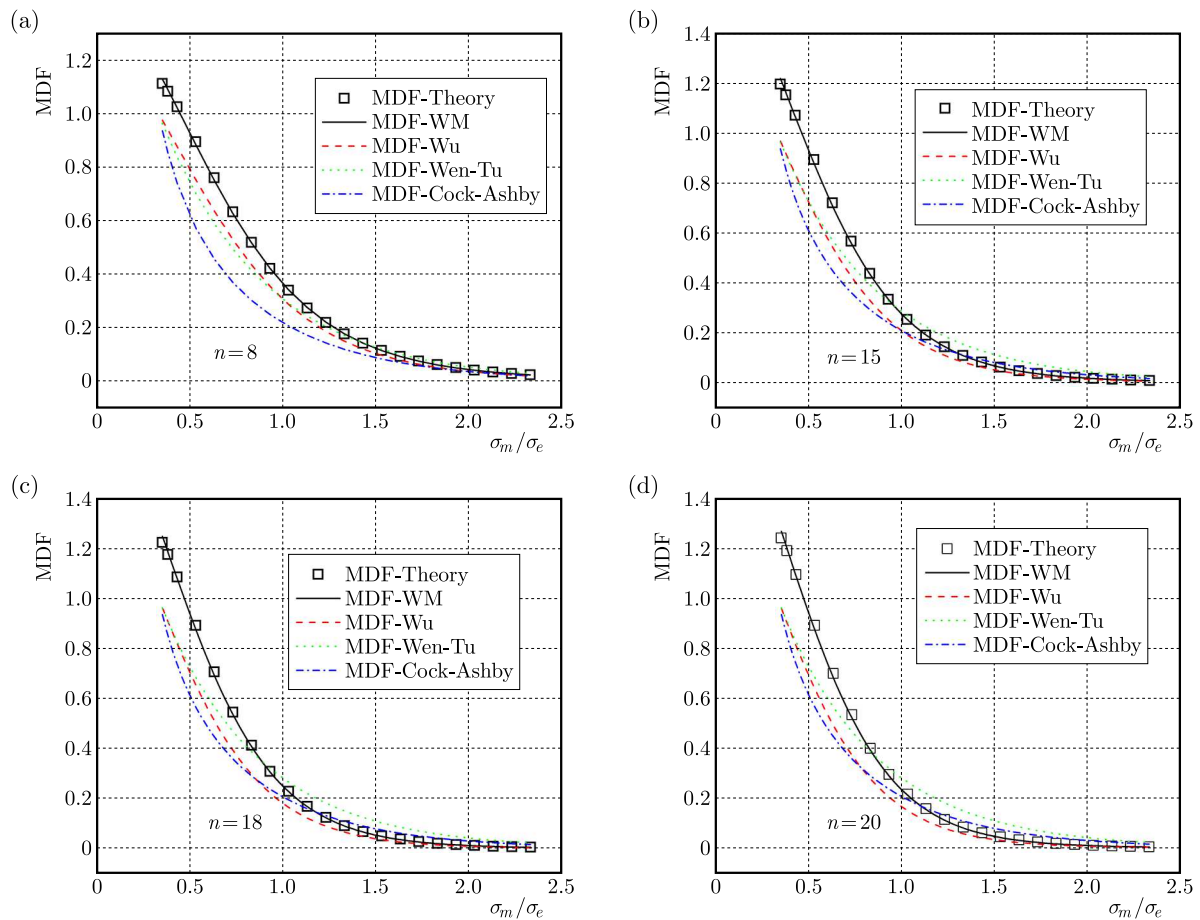
Fig. 6. Comparison of predictions and theoretical results of *MDF*

Figure 7 shows the influence of stress triaxiality on the multiaxial ductility factor. The data for steels of the pipe and rotor are collected from Wichtmann (2002), and the data for C-Mn steel at 360°C from Yatomi *et al.* (2004), 316H at 550°C (Wen and Tu, 2014) and for 316 type steel at 600°C (Spindler, 2004b). As presented in Fig. 7, the Cocks-Ashby model may underestimate the multiaxial creep ductility at high stress triaxiality, while the Wen-Tu and Wu models give more closer results to the experimental data and may become close to the average results of tested data. The WM model gives more improved solutions at small stress triaxiality while more conservative predictions at higher stress state. This is due to theoretical solutions of the WM model, which indeed have these variation laws as observed in Fig. 7, and which may be larger than the predictions of the other three models at low stress triaxiality but may be less than these predictions at high stress triaxiality. In general, it could be said that the new Wu and WM models could give better predictions for the multiaxial ductility factor compared to the previous models. The WM model may give a more precise upper bound of *MDF* for pipe and rotors steel as well as for 316 steel at 600°C, while WM predictions are also effectively consistent with the average experimental results for C-Mn steel at 360°C and 316H at 550°C.
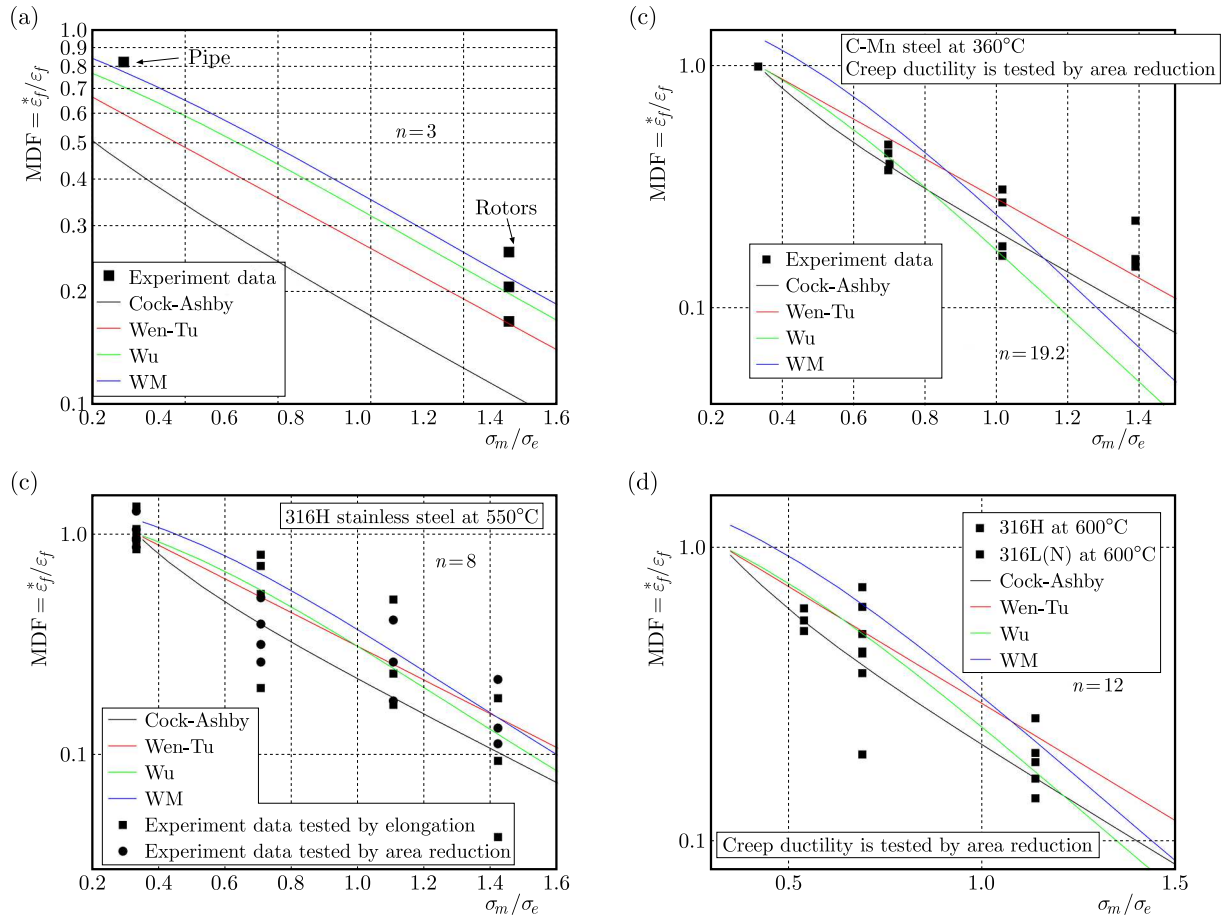
Fig. 7. Comparison of predictions and experimental data of *MDF*: (a) for pipe and rotors, (b) for C-Mn steel at 360°C, (c) for 316H at 550°C, (d) for 316H(L) at 600°C

Figure 8 compares the predictions by using different models and experimental data of the multiaxial ductility factor. The experimental data under the same stress triaxiality are simplified by calculating the geometric mean values. It could be found for these limited data for different materials and conditions, all predictions of the Cocks-Ashby model could be located within the range with a scatter factor of 2, and for the Wen-Tu and Wu models, this error band is with a scatter factor of 1.8 and 1.6, respectively. For the WM model, the predictions are located within the range with a scatter factor of 1.4. This demonstrates the accuracy of the WM model in predicting *MDF* based on growth of grain-boundary cavities by a power-law creep.

3. Conclusion

In this study, the multiaxial ductility factor was analyzed and two novel predicting models were developed based on the power-law creep grain-boundary cavities growth theory under multiaxial stress states proposed by Cocks and Ashby. The details are summarized as follows.

- The predicting model of stress-state parameter α was revised by using an empirical equation denoted as α_{Wu}, and the relationship between uniaxial and multiaxial creep failure strain could be obtained, then an empirical multiaxial ductility factor MDF_{Wu} was built by using α_{Wu}.
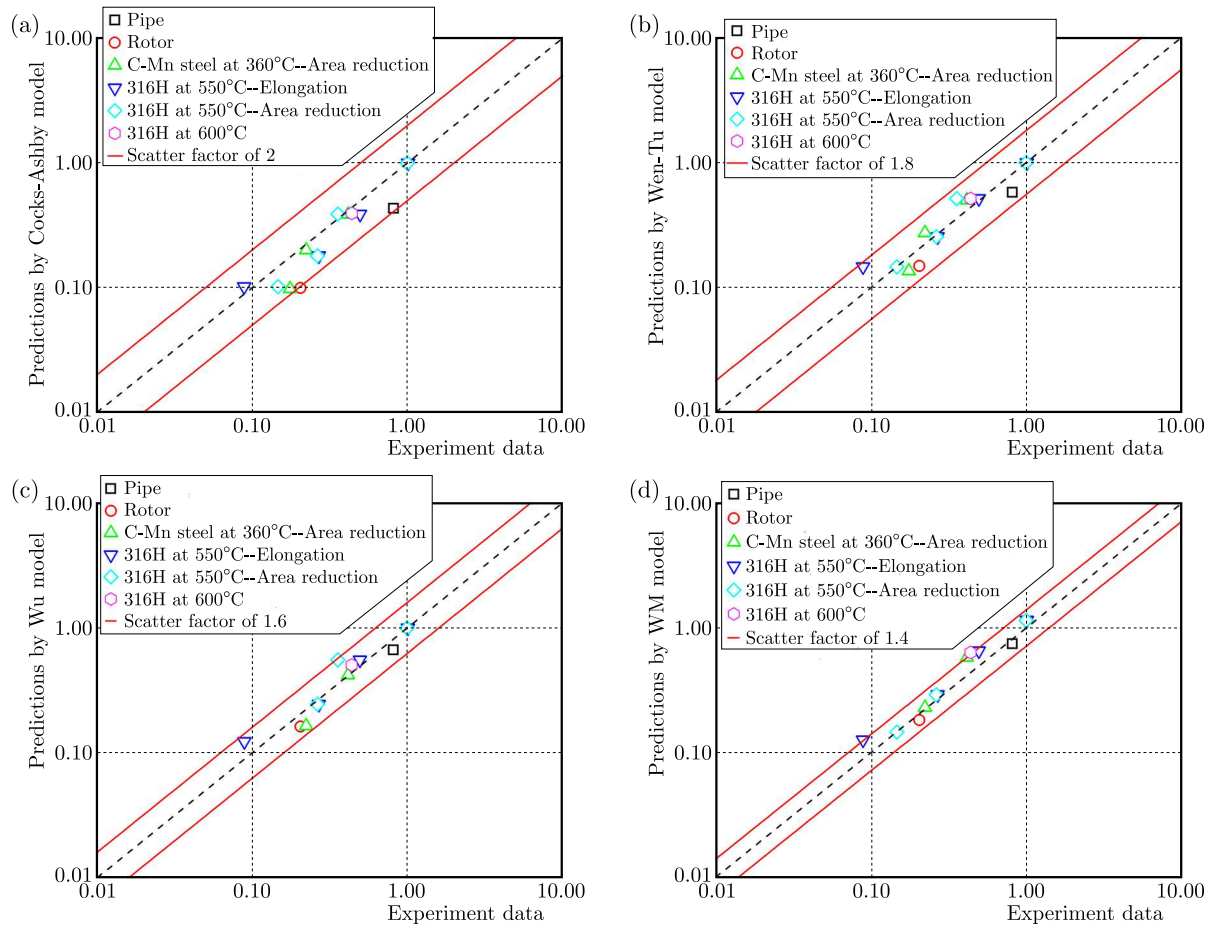
Fig. 8. Comparison of predictions and experimental data of *MDF*: (a) for Cocks-Ashby model, (b) for Wen-Tu model, (c) for Wu model, (d) for WM model

- The theoretical expression for multiaxial ductility factor *MDF* could also be established. By fitting theoretical curves of *MDF* against stress traiaxiality σ_m/σ_{eq}, another predicting model MDF_{WM} could be developed.
- Predictions of these two novel multiaxial ductility factor models as well as C-A and W-T models were compared with experimental data. The accuracy of MDF_{Wu} and MDF_{WM} models was obviously enhanced, especially for the MDF_{WM} with a scatter factor of only 1.4.

References

1. ALANG N.A., NIKBIN K., 2018, An analytical and numerical approach to multiscale ductility constraint based model to predict uniaxial/multiaxial creep rupture and cracking rates, *International Journal of Mechanical Sciences*, **135**, 342-352

2. AL-RIFAIE H., STUDZIŃSKI R., GAJEWSKI T., MALENDOWSKI M., SUMELKA W., SIELICKI P.W., 2021, A new blast absorbing sandwich panel with unconnected corrugated layersnumerical study, *Energies*, **14**, 1

3. AL-RIFAIE H., SUMELKA W., 2019, The development of a new shock absorbing uniaxial graded auxetic damper (UGAD), *Materials*, **12**, 16

4. COCKS A.C.F., ASHBY M.F., 1980, Intergranular fracture during power-law creep under multi-axial stresses, *Metal Science Journal*, **14**, 8-9, 395-402

5. DAVIES C., 2006, *Crack Initiation and Growth at Elevated Temperatures in Engineering Steels*, Imperial College London

6. HOLDSWORTH S.R., 1992, Initiation and early growth of creep cracks from pre-existing defects, *Materials at High Temperatures*, **10**, 2, 127-137

7. MANJOINE M.J., 1975, Ductility indices at elevated temperature, *Journal of Engineering Materials and Technology*, **97**, 2, 156-161

8. McCLINTOCK F.A., 1968, A criterion for ductile fracture by the growth of holes, *Journal of Applied Mechanics*, **35**, 2, 363-371

9. RICE J.R., TRACEY D.M., 1969, On the ductile enlargement of voids in triaxial stress fields, *Journal of the Mechanics and Physics of Solids*, **17**, 3, 201-217

10. SPINDLER M.W., 2004a, The multiaxial and uniaxial creep ductility of Type 304 steel as a function of stress and strain rate, *Materials at High Temperatures*, **21**, 1, 47-54

11. SPINDLER M.W., 2004b, The multiaxial creep ductility of austenitic stainless steels, *Fatigue and Fracture of Engineering Materials and Structures*, **27**, 4, 273-281

12. SPINDLER M.W., HALES R., SKELTON R.P., 2001, Multiaxial creep ductility of an ex-service type 316 H stainless steel, *9th International Conference on Creep and Fracture of Engineering Materials and Structure*, 679-688

13. TAN J.P., TU S.T., WANG G.Z., XUAN F.Z., 2013, Effect and mechanism of out-of-plane constraint on creep crack growth behavior of a Cr-Mo-V steel, *Engineering Fracture Mechanics*, **99**, 324-334

14. WEN J.F., TU S.T., 2014, A multiaxial creep-damage model for creep crack growth considering cavity growth and microcrack interaction, *Engineering Fracture Mechanics*, **123**, 197-210

15. WEN J.F., TU S.T., XUAN F.Z., ZHANG X.W., GAO X.L., 2016, Effects of stress level and stress state on creep guctility: evaluation of different models, *Journal of Materials Science and Technology*, **32**, 8, 695-704

16. WICHTMANN A., 2002, Evaluation of creep damage due to void growth under triaxial stress states in the design of steam turbine components, *JSME International Journal*, **45**, 1, 72-76

17. WU D., JING H., XU L., 2020, Engineering application of enhanced C*-Q* two parameter approaches for predicting creep crack initiation times, *European Journal of Mechanics – A/Solids*, **82**, 104013

18. WU D., JING H., XU L., ZHAO L., HAN Y., 2018a, Analytical approaches of creep crack initiation prediction coupled with the residual stress and constraint effect, *European Journal of Mechanics – A/Solids*, **71**, 1-15

19. WU D., JING H., XU L., ZHAO L., HAN Y., 2018b, Numerical analysis of the creep crack constraint effects and the creep crack initiation for pressurized pipelines with circumferential surface cracks, *Advances in Engineering Software*, **115**, 40-51

20. WU D., JING H., XU L., ZHAO L., HAN Y., 2018c, Theoretical and numerical analysis of the creep crack initiation time considering the constraint effects for pressurized pipelines with axial surface cracks, *International Journal of Mechanical Sciences*, **141**, 262-275

21. WU D., JING H., XU L., ZHAO L., HAN Y., 2018d, Theoretical and numerical analysis of creep crack initiation combined with primary and secondary stresses, *Theoretical and Applied Fracture Mechanics*, **95**, 143-154

22. WU D., JING H., XU L., ZHAO L., HAN Y., 2018e, Two-parameter approach of creep crack initiation times considering the constraint effect induced by specimen geometry, *Theoretical and Applied Fracture Mechanics*, **96**, 31-44

23. WU D., JING H., XU L., ZHAO L., HAN Y., 2019, Enhanced models of creep crack initiation prediction coupled the stress-regime creep properties and constraint effect, *European Journal of Mechanics – A/Solids*, **74**, 145-159

24. YATOMI M., BETTINSON A.D., O'DOWD N.P., NIKBIN K.M., 2004, Modelling of damage development and failure in notched-bar multiaxial creep tests, *Fatigue and Fracture of Engineering Materials and Structures*, **27**, 4, 283-295

25. YATOMI M., TABUCHI M., 2010, Issues relating to numerical modelling of creep crack growth, *Engineering Fracture Mechanics*, **77**, 15, 3043-3052

26. YOU B.R., LEE S.B., 1996, A critical review on multiaxial fatigue assessments of metals, *International Journal of Fatigue*, **18**, 4, 235-244